Cell Reports

Report

High Plasticity of New Granule Cells in the Aging Hippocampus

Graphical Abstract

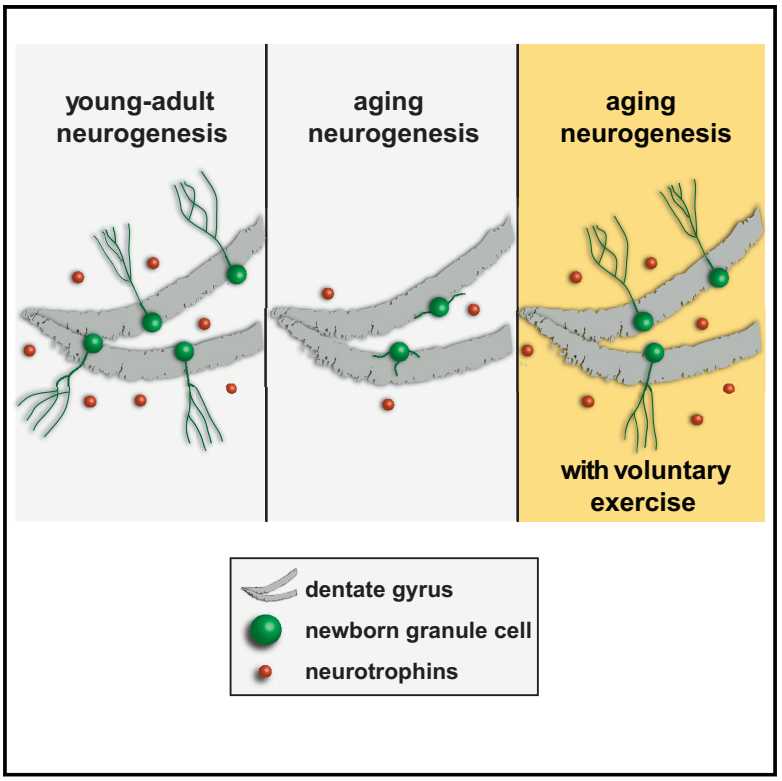

Authors

Mariela F. Trinchero, Karina A. Buttner, Jessica N. Sulkes Cuevas, ..., Fernanda Ledda, Gustavo Paratcha, Alejandro F. Schinder

Correspondence

aschinder@leloir.org.ar

In Brief

Trinchero et al. show that development of new granule cells born in the adult hippocampus is strongly influenced by age. In the aging hippocampus, new neurons remain immature for prolonged intervals, yet voluntary exercise triggers their rapid growth and functional synaptogenesis. This extensive structural remodeling is mediated by neurotrophins.

Highlights

- In the aging hippocampus, development of new granule cells is largely retarded
- Running promotes the rapid integration of new neurons in the aging brain
- The effects of running require neurotrophin signaling
- Plasticity of aging networks is maximized by exercise and neurotrophins

Trinchero et al., 2017, Cell Reports *21*, 1129–1139
October 31, 2017
https://doi.org/10.1016/j.celrep.2017.09.064

CellPress

Cell Reports
Report

High Plasticity of New Granule Cells in the Aging Hippocampus

Mariela F. Trinchero,[1] Karina A. Buttner,[1] Jessica N. Sulkes Cuevas,[1] Silvio G. Temprana,[1] Paula A. Fontanet,[2] M. Cristina Monzón-Salinas,[1] Fernanda Ledda,[2] Gustavo Paratcha,[2] and Alejandro F. Schinder[1,3,*]
[1]Laboratorio de Plasticidad Neuronal, Fundación Instituto Leloir, Instituto de Investigaciones Bioquímicas de Buenos Aires, Consejo Nacional de Investigaciones Científicas y Técnicas (CONICET), Av. Patricias Argentinas 435, Buenos Aires C1405BWE, Argentina
[2]División de Neurociencia Celular y Molecular, Instituto de Biología Celular y Neurociencias (IBCN-CONICET-UBA), Facultad de Medicina, Paraguay 2155, Buenos Aires C1121ABG, Argentina
[3]Lead Contact
*Correspondence: aschinder@leloir.org.ar
https://doi.org/10.1016/j.celrep.2017.09.064

SUMMARY

During aging, the brain undergoes changes that impair cognitive capacity and circuit plasticity, including a marked decrease in production of adult-born hippocampal neurons. It is unclear whether development and integration of those new neurons are also affected by age. Here, we show that adult-born granule cells (GCs) in aging mice are scarce and exhibit slow development, but they display a remarkable potential for structural plasticity. Retrovirally labeled 3-week-old GCs in middle-aged mice were small, underdeveloped, and disconnected. Neuronal development and integration were accelerated by voluntary exercise or environmental enrichment. Similar effects were observed via knockdown of Lrig1, an endogenous negative modulator of neurotrophin receptors. Consistently, blocking neurotrophin signaling by Lrig1 overexpression abolished the positive effects of exercise. These results demonstrate an unparalleled degree of plasticity in the aging brain mediated by neurotrophins, whereby new GCs remain immature until becoming rapidly recruited to the network by activity.

INTRODUCTION

Aging is a multifaceted process that affects the physiological integrity of cells, tissues, and organs, ultimately deteriorating the quality of life (Guarente, 2014; López-Otín et al., 2013). Age constitutes a primary risk factor for major human pathologies, including neurodegenerative disorders such as Alzheimer's and Parkinson's diseases, characterized by the progressive loss of specific neuronal populations (Irwin et al., 2013; Mattson, 2012). Even in the healthy brain, aging typically impairs cognitive abilities, the speed of information processing, and the capacity for memory formation and retention. These changes are associated with decreased connectivity rather than neuronal loss. Neural circuits become affected by senescence at the molecular, cellular, and network levels, displaying decreased synapse numbers, synaptic proteins, and neurotransmitter receptors, with concomitant alterations in transmission and plasticity (Burke and Barnes, 2010; Fan et al., 2017). Plasticity is what allows the brain to adapt to novel stimuli to produce an adaptive behavior. In the dentate gyrus of the hippocampus, plasticity is not limited to synaptic remodeling, but it also includes the production of new granule cells (GCs) that develop and integrate in the preexisting circuits, producing substantial modifications in local networks that contribute to the capacity for the discrimination of subtle contextual differences (Kropff et al., 2015; Lepousez et al., 2015).

In the aging hippocampus, numbers of excitatory synapses decrease, and contacts lose their ability to undergo activity-dependent, long-term potentiation required for proper memory formation and for the establishment of spatial maps. Thus, the capacity of neural circuits to respond and adapt to challenges from the external world by modifying specific synaptic connections becomes impaired (Burke and Barnes, 2010). Hippocampal neurogenesis is also greatly diminished by age (Kempermann et al., 1998; Kuhn et al., 1996; Kuipers et al., 2015), and multiple mechanisms seem to be responsible for loss of plasticity. Aging affects cell-intrinsic pathways that reduce self-renewal of neural stem cells, their neurogenic capacity, and the survival of newly generated neurons both in the dentate gyrus and the subventricular zone (Beckervordersandforth et al., 2017; Corenblum et al., 2016; Encinas et al., 2011; Knobloch et al., 2013; Kuipers et al., 2015; Moore et al., 2015). Extrinsic signals also play critical roles in the decline of adult neurogenesis observed in the aging brain (Fan et al., 2017; Villeda et al., 2011). The age-dependent decline in hippocampal neurogenesis has been proposed as a possible mechanism contributing to cognitive impairment.

Among the several remaining questions about the regulation of adult neurogenesis, it is unclear whether newly generated GCs integrate properly in the context of the aging hippocampus (Burke and Barnes, 2010; Fan et al., 2017; Mattson, 2012). Not only does integration depend on proper neuronal differentiation of stem cells, migration, and growth, but it also demands the establishment of synaptic connections and the possibility to refine those connections in an activity-dependent manner, which highlights the complexity of the neurogenic process in the adult brain. Thus, new GCs might serve as suitable probes to interrogate the capacity of the aging brain to undergo all of these steps successfully. Because development and integration of adult-born GCs are sensitive to subtle modifications that impinge on

the activity of the local niche (Alvarez et al., 2016; Piatti et al., 2011), here, we have hypothesized that the multiple alterations found in the aging brain affect not only the quantity but also the quality and functionality of the neurogenic process. We have also tested whether GCs born in aging mice are responsive to conditions that are known to enhance brain health and plasticity.

RESULTS

Delayed Development of Adult-Born Neurons in the Aging Dentate Gyrus

As a first approach to investigate the impact of age, we analyzed morphological development of new GCs generated in the septal hippocampus of young adult, adult, and middle-aged mice (2, 5, and 8 months old; 2M, 5M, and 8M mice, respectively). Adult-born GCs were labeled using a retroviral construct expressing GFP and analyzed by confocal imaging at different days post-injection (dpi), which accurately represents the developmental age of the labeled neuron (Figures 1A–1C). Besides the well-known fact that the number of new GCs decreases in aging animals, we noted that GCs generated in 5M and 8M mice displayed shorter and simpler dendrites than those generated in 2M mice, particularly at early stages of development (<4 weeks). These features were reflected in the shorter dendritic length and reduced number of branches (Figure 1D). Notably, 21-dpi GCs had reached an almost mature morphology in 2M mice but looked incipient in 8M mice. Overall, dendritic growth curves were shifted to the right in older mice, but eventually, GCs born at all ages showed similar dendritic features upon reaching the plateau phase (Figures 1C and 1D).

Synaptic integration of developing GCs follows a stereotyped sequence that has been widely validated, starting with the formation of GABAergic dendritic inputs and followed by glutamatergic synaptogenesis several days later, which is accompanied by the formation of dendritic spines (Chancey et al., 2013; Espósito et al., 2005; Ge et al., 2006; Piatti et al., 2011; Zhao et al., 2006). In the young adult brain, dendritic spine density in new GCs increased abruptly by the third week and showed a peak at 28 dpi that decreased with neuronal age until reaching a plateau (Figures 1E and 1F). Such an increase in spine number was delayed in older mice. In particular, while 21-dpi GCs from 2M mice displayed ~1.5 spines per micrometer, those in 8M mice displayed no spines along their dendritic shafts, suggesting a complete lack of glutamatergic connectivity. At all ages, a sharp increase in spine formation was observed from 21- to 28-dpi GCs, and similar spine density values were reached upon maturation. Together, these observations suggest that age induces a developmental delay in adult born GCs.

Physical Exercise Promotes the Rapid Functional Integration of New GCs

Physical exercise exerts positive effects at multiple levels in the aging brain, improving metabolic parameters and, ultimately, memory and cognitive performance (Duzel et al., 2016; Mattson, 2012). In mice exposed to a running wheel, these effects correlate with an increase in the production of new GCs (Marlatt et al., 2012; van Praag et al., 1999, 2005). In young adult mice, the development and integration of adult-born GCs are also shaped by physical exercise and experience, which adds additional levels of activity-dependent plasticity to network remodeling by neurogenesis (Alvarez et al., 2016; Bergami et al., 2015; Piatti et al., 2011). To test whether developing GCs in the aging brain respond to physiological stimuli, we analyzed the effects of voluntary exercise (running) in 8M mice. Surprisingly, running increased the proportion of GCs expressing the mature neuronal marker calbindin (Cb) by more than 3-fold in 21-dpi GCs, reflecting an accelerated development (Figures 2A–2C). In addition, GCs in running mice displayed morphological properties typical of mature neurons, with complex dendritic trees bearing long and ramified dendrites, about 4-fold longer than those of the largely immature GCs in sedentary mice (Figures 2D–2F). Dendrites in running mice were now coated with spines at a high density both in the middle and outer molecular layers (~2/μm), which suggests that neurons have already established connections with the host network (Figure 2G). Overall, 21-dpi GCs in running mice at 8M acquired similar structural features as new neurons in young adult mice (2M; Figure S1). It is interesting to note that, even though the degree of maturation reached at 21 dpi under sedentary conditions was different at each age studied, all GCs in running mice achieved similar morphology regardless of the mouse's age (2M, 5M, and 8M) (Figure S1).

To monitor possible changes in functional connectivity that may accompany the structural remodeling triggered by voluntary exercise, electrophysiological recordings were carried out in 21-dpi GCs in acute slices obtained from sedentary and running middle-aged (12M) mice. GCs from sedentary mice displayed high membrane resistance, a lack of action potentials, and an absence of spontaneous excitatory postsynaptic currents (sEPSCs), indicative of an incipient neuronal phenotype lacking functional glutamatergic synaptic inputs (Figures 2H–2J). In striking contrast, new GCs from running mice fired repetitively and showed spontaneous glutamatergic postsynaptic currents, which demonstrates that they have been integrated in the local circuits. Despite being more connected, new GCs from running mice still displayed high input resistance, few spikes, and low sEPSC frequency, which indicate that they have not yet reached functional maturity (Espósito et al., 2005; Mongiat et al., 2009). Together, these data demonstrate that GCs developing in older mice exhibit a remarkable sensitivity to hippocampal activation by voluntary exercise, which elicits structural and functional changes needed to recruit new neurons to the network.

Because exploration of an enriched environment (EE) generates reliable local activity that promotes synaptic plasticity and the integration of new GCs in the temporal hippocampus in young adult mice (Alvarez et al., 2016; Chancey et al., 2013), we decided to test its modulatory effects in middle-aged mice (Figures 3A and 3B). An EE produced substantial acceleration of new GC integration in 8M mice (Figures 3C–3F). GCs from stimulated mice displayed longer and more complex dendritic trees, with variable extents of responsiveness in all analyzed mice. When examined in detail, they presented dendritic spines reflecting connections to glutamatergic afferents from the perforant path. Although this modulation was somewhat weaker than the one elicited by running, these results indicate that new GCs can also respond to exploratory experience with accelerated integration.

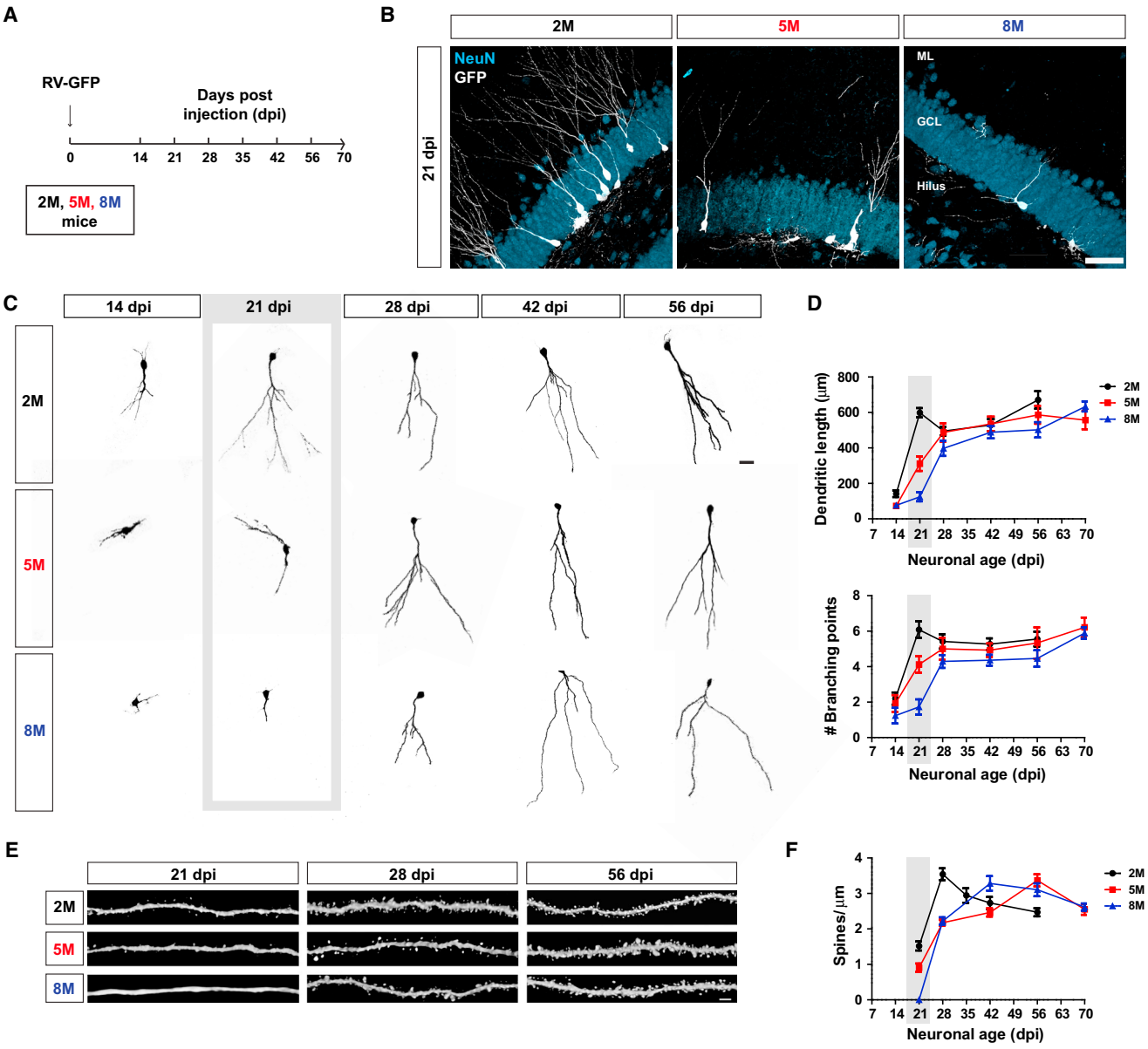

Figure 1. Age-Dependent Delay in Morphological Development of Adult-Born GCs

(A) Experimental design. RV-GFP was infused in the right dentate gyrus of 2M, 5M, and 8M mice. Neuronal morphology was analyzed at different times after immunofluorescence and confocal imaging.

(B) Representative images of 21 dpi GCs expressing GFP (white) taken at the indicated mouse age. NeuN (blue) labels the granule cell layer (ML, molecular layer; GCL, granule cell layer). Scale bar, 40 μm.

(C) Representative images of new GCs at different developmental ages obtained from 2M, 5M, and 8M mice. Individual neurons have been cropped from original images. Scale bar, 20 μm.

(D) Quantification of dendritic complexity (length and branching points) versus neuronal age for the indicated mouse ages. Data were obtained from 10 to 28 neurons (3 to 5 mice per point). Statistical significance for 21 dpi; dendritic length: 2M versus 5M and 2M versus 8M, $p < 0.001$; 5M versus 8M, $p < 0.01$; branching points: 2M versus 5M, $p < 0.05$; 2M versus 8M, $p < 0.001$; 5M versus 8M, $p < 0.01$.

(E) Dendritic segments from newborn GCs at the indicated times. Scale bar, 2 μm.

(F) Spine density measured from 10 to 24 neurons (3 to 5 mice per point). Statistical significance for 21 dpi; 2M versus 8M $p < 0.001$, 5M versus 8M, $p < 0.01$. In (D) and (F), dots connected by straight lines denote means, and error bars denote SEM.

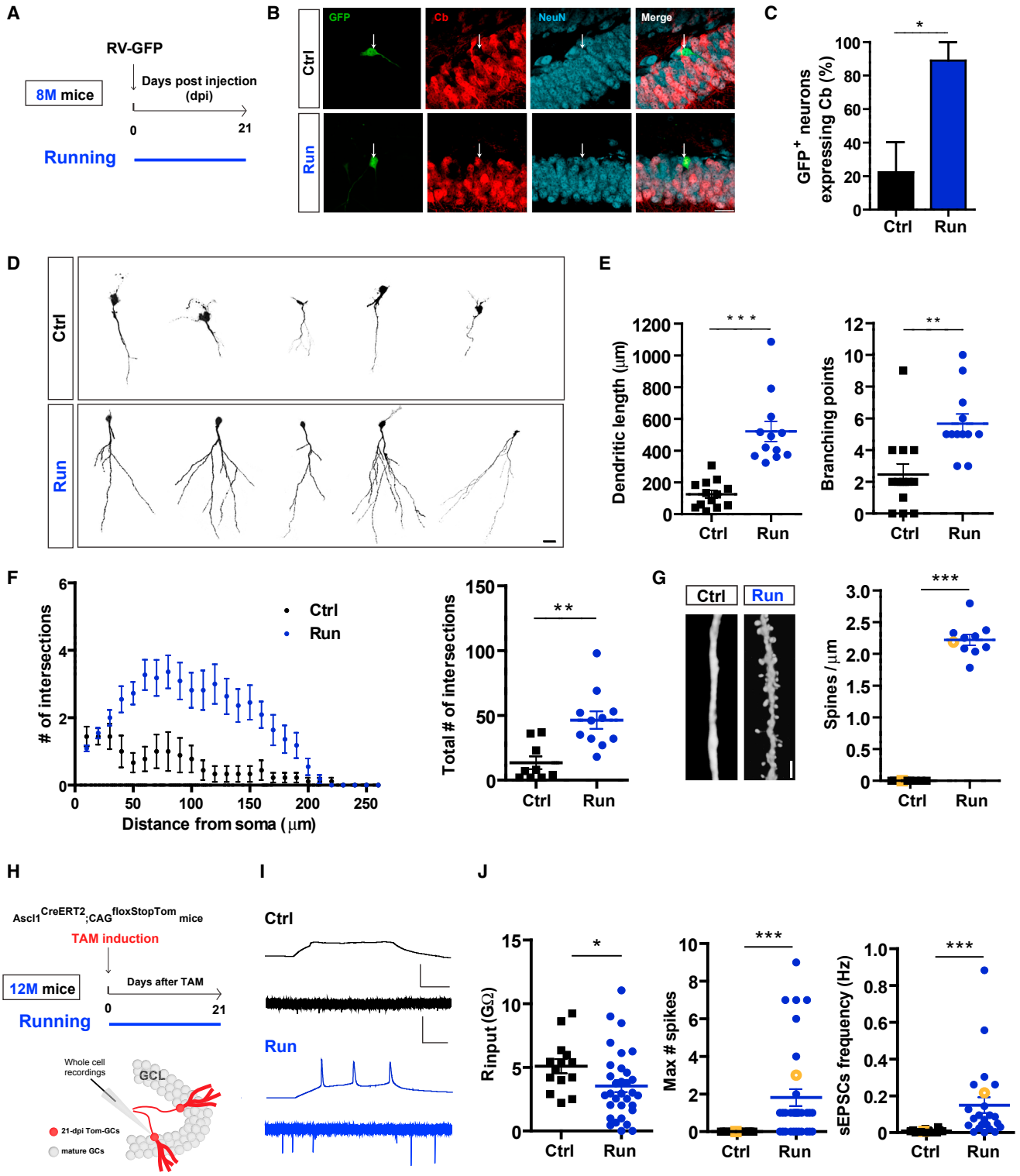

Figure 2. Voluntary Exercise Promotes the Rapid Integration of New GCs Born in 8M mice

(A–G) Morphological analysis. (A) RV-GFP was infused in the right dentate gyrus of 8M mice. Mice were housed with (Run) or without a running wheel (Ctrl) for 21 days (blue segment). Morphological analysis was done on GFP-GCs at 21 dpi. (B) Single optical planes for example GCs (green, indicated by the arrow) from a sedentary mouse and a running mouse, displaying the expression of NeuN (blue) and Cb (red). Scale bar, 20 µm. (C) Cb expression in new GCs from control and running mice. *$p < 0.05$ after t test with Welch's correction, with n = 29 (Ctrl) and 20 neurons (Run) from 3–4 mice. (D) Representative images of 21-dpi GFP-GCs.

(legend continued on next page)

Mechanisms Responsible for Running-Mediated Neuronal Integration in the Aging Brain

In young adult mice, dendritic development of adult-born GCs has been shown to rely on neurotrophin signaling through a mechanism that involves autocrine secretion (Bergami et al., 2008; Wang et al., 2015; Waterhouse et al., 2012). Each step of the neurotrophin signaling pathway—including synthesis, secretion, and action—is optimized by neuronal activity (McAllister et al., 1996; Meyer-Franke et al., 1998; Park and Poo, 2013). In the aging hippocampus, the delayed development of new GCs correlated with a decrease in the activity of the granule cell layer and a decline in the levels of brain-derived neurotrophic factor (BDNF) protein (Figure S2). Moreover, running increased activity in the granule cell layer and enhanced hippocampal BDNF levels in 8M mice (Figure S3) (Adlard et al., 2005; Marlatt et al., 2012; Oliff et al., 1998; Piatti et al., 2011). We hypothesized that the effect of running observed here might involve the combined effects of neurotrophin release enhanced by overall activity and downstream effects boosted by intrinsic neuronal depolarization. We thus tested their individual contributions.

To enhance the activity of developing GCs in a cell-intrinsic manner, we used a retrovirus to express the synthetic G-protein-coupled receptor hM3Dq together with a fluorescent reporter (RV-EGFP-hM3Dq), which elicits neuronal depolarization upon binding to the synthetic ligand clozapine-N-oxide (CNO) (Alexander et al., 2009; Alvarez et al., 2016; Sternson and Roth, 2014; Temprana et al., 2015). Chronic activation of hM3Dq-expressing GCs from 8M mice resulted in significant dendritic growth (Figures 3G–3J). Consistent with the notion that increased intrinsic activity might counteract the age-dependent reduction in the activation of the granule cell layer, the accelerated growth observed after chronic stimulation of hM3Dq-expressing GCs was also age dependent, with the largest effect occurring in new GCs of 8M mice (Figures S4A–S4F).

To modulate neurotrophin signaling in a cell-intrinsic manner, we aimed to knockdown Lrig1, an endogenous negative modulator of tyrosine kinase receptors—including neurotrophin receptors—which controls dendritic morphogenesis in the developing and adult hippocampus (Alsina et al., 2016; Bergami et al., 2008; Cheung et al., 2007). We used a retrovirus (RV) to express a short hairpin RNA (shRNA) for Lrig1 together with GFP (RV-shLrig1-EGFP) in new GCs of 8M mice and analyzed their morphology after 3 weeks (Figures 4A–4D). Lrig1 downregulation mimicked the effects observed by activity and experience in developing GCs, favoring neuronal maturation in a manner that is enhanced at older ages (Figures 4C, 4D, and S4). The results presented thus far show that the aging hippocampus progresses toward a reduction in overall neuronal activity and neurotrophin availability, and both factors influence when and how newly generated GCs mature and integrate.

The striking growth induced by running in 21-dpi GCs (8M mice) suggested a ceiling effect over dendritogenesis, probably due to the cumulative influence of prolonged exercise on developing cells. To better understand the interaction between exercise and neurotrophin signaling, we searched for experimental conditions that would allow positive modulation. Cumulative effects would be limited in younger neurons. Consistent with this notion, GCs at 14 dpi were not affected by running or by Lrig1 knockdown (Figures 4E–4G). In contrast, the simultaneous combination of both stimuli duplicated the extension of dendritic processes. Thus, 14-dpi GCs in 8M mice that received these combined stimuli showed longer dendrites (204 μm ± 33 μm) than same-age neurons in 2M mice (149 μm ± 30 μm; compare to Figures 1C and 1D). This was the only condition where GCs from middle-aged mice displayed more mature features than neurons of the same age in young mice. Taken together, these results suggest that neurotrophin signaling might be a key mediator linking activity and cell growth in aging mice.

To confirm this hypothesis, we investigated whether attenuating neurotrophin function in a cell-intrinsic manner would modify the responsiveness of developing GCs to voluntary exercise. It was recently shown that Lrig1 overexpression can reduce dendritic growth induced by BDNF in developing hippocampal neurons (Alsina et al., 2016). We used a retrovirus to overexpress Lrig1 (RV-GFP-*oe*Lrig1) in newly generated GCs in middle-aged mice and analyzed the effects of running (Figures 5A–5C). Notably, *oe*Lrig1 completely abolished dendritic growth in running mice. These results demonstrate that neurotrophins mediate the accelerated integration of new neurons induced by exercise in the aging brain.

DISCUSSION

The aging brain exhibits a marked reduction in the rate of adult hippocampal neurogenesis (Kempermann et al., 1998; Kuhn et al., 1996; Kuipers et al., 2015; Morgenstern et al., 2008). Such decline has been attributed to a decrease in the size of the neural stem cell pool, but its causes continue to be investigated (Bonaguidi et al., 2011; Encinas et al., 2011; Sierra et al., 2015). We now report that

Scale bar, 20 μm. Individual neurons have been cropped from original images. (E and F) Dendritic measurements (E) and Sholl analysis (F) of GFP-GCs. $^{**}p < 0.01$ and $^{***}p < 0.001$ after t test with Welch's correction, with n = 11 (Ctrl) and 12 GCs (Run) from 4 mice. (G) Spines observed in dendritic segments from GFP-GCs. Scale bar, 2 μm. $^{***}p < 0.001$ after t test with Welch's correction, with n = 10 segments from 5 mice for each condition. Orange dots correspond to displayed segments. In (F), dots denote means, and error bars denote SEM. In (H)–(J), the functional properties of new GCs from control and running 12M mice are indicated.

(H) Experimental design. Ascl1^{CreERT2};CAG^{floxStopTom} mice received TAM to label new GCs and were housed with (Run) or without (Ctrl) a running wheel. Whole-cell recordings were carried out at 21 dpi in Tom-GCs in acute slices.

(I) Top: representative membrane potential responses to depolarizing current steps (10 pA, 200 ms) for control (Ctrl) and running (Run) mice. Scale bars, 25 mV, 60 ms. Bottom: representative current traces depicting sEPSCs obtained from Tom-GCs held at −70 mV. Scale bars, 20 pA, 5 s.

(J) Left: input resistance in Tom-GCs. $^{*}p < 0.05$ after Mann-Whitney's test with n = 14 (Ctrl) and 27 neurons (Run). Center: maximum number of spikes elicited by depolarizing current steps. Right: sEPSC frequency. $^{***}p < 0.001$ after Mann-Whitney test with n = 24 (Ctrl) and 23 neurons (Run) from 4 to 5 mice. Orange circles correspond to example traces shown in (I).

In (C), (E)–(G) and (J) central horizontal bars denote means and error bars denote SEM.

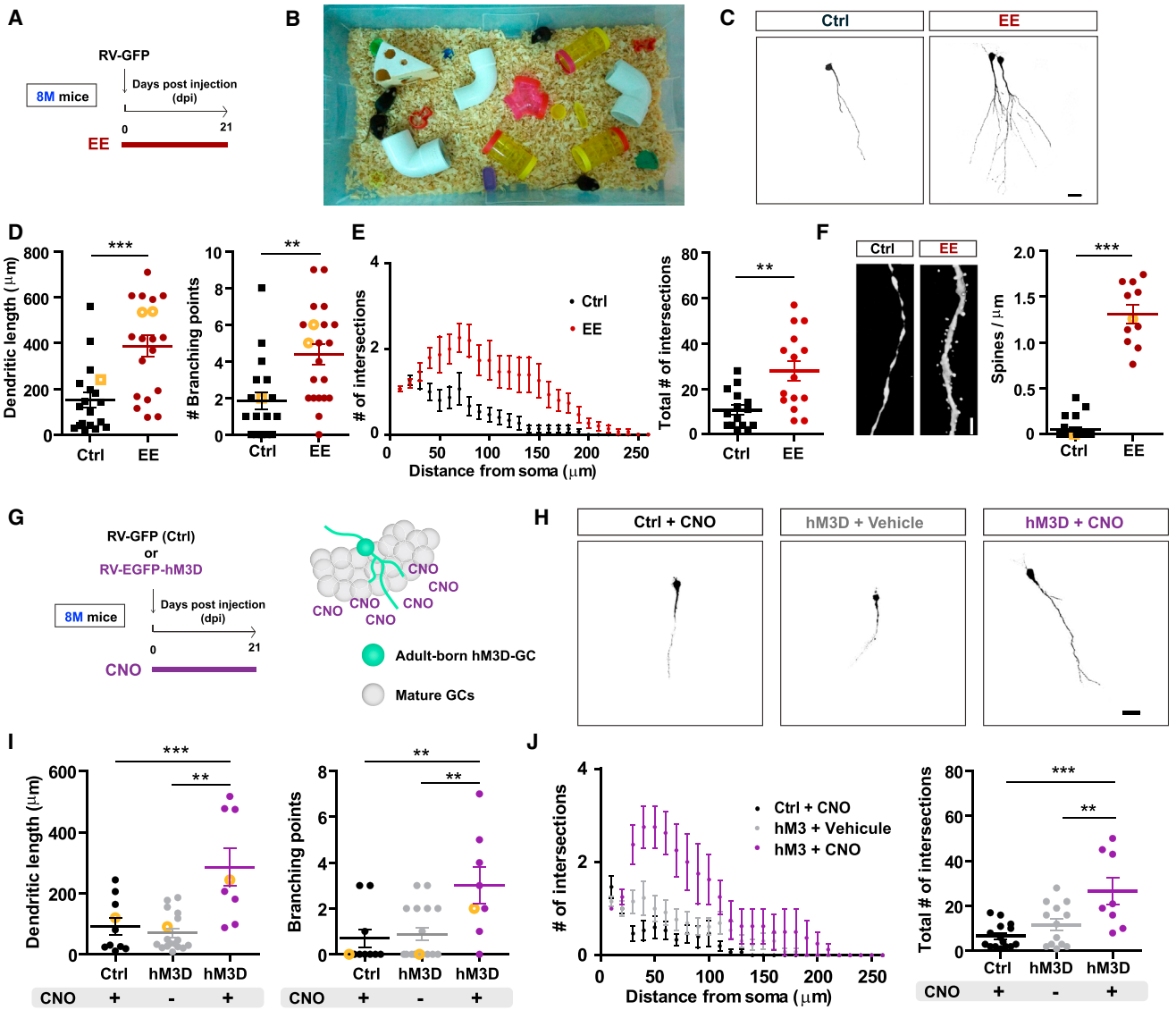

Figure 3. GC Maturation in Middle-Aged Mice Is Accelerated by EE and Intrinsic Chemogenetic Activation

(A–F) Effects of EE in 21 dpi GFP-GCs. (A) RV-GFP was infused in 8M mice housed in control or EE conditions for 21 days (red segment). GC morphology was analyzed by immunofluorescence and confocal microscopy. (B) Example of EE. (C) Representative images of 21-dpi GCs obtained from control and EE mice. Scale bar, 20 μm. Individual neurons have been cropped from original images. (D and E) Dendritic measurements (D) and Sholl analysis (E) of GFP-GCs. $^{**}p < 0.01$ and $^{***}p < 0.001$ after t test with Welch's correction, with n = 19 neurons from 4 mice for each condition. (F) Segments from GFP-GCs highlighting dendritic spines and their corresponding quantifications. Scale bar, 2 μm. $^{***}p < 0.001$ after t test with Welch's correction, with n = 20 (Ctrl) and 11 dendritic segments (EE) from 5 mice.

(G–J) Chemogenetic intrinsic activation of new GCs. (G) Experimental design. RV-hM3D-EGFP or RV-GFP (Ctrl) was used to transduce new GCs (hM3D-GCs) in 8M mice. Mice received CNO (purple segment) or vehicle for 21 days to stimulate hM3D-GCs. Morphological analysis was done at 21 dpi. (H) Representative images of 21-dpi GCs at the indicated conditions. Individual neurons have been cropped from original images. Scale bar, 20 μm. (I) Dendritic measurements. $^{**}p < 0.01$ and $^{***}p < 0.001$ after ANOVA followed by Bonferroni post hoc test, with n = 10 (Ctrl), 17 (hM3D), and 8 GCs (hM3D + CNO) from 4 mice. Orange symbols correspond to example neurons shown in (G). (J) Sholl analysis for the data shown in (H) and (I), where $^{**}p < 0.01$ and $^{***}p < 0.001$ after Kruskal-Wallis test followed by Dunn post hoc test.

Horizontal and error bars denote mean ± SEM.

development and functional integration of new GCs occur at a much slower pace in middle-aged than in young adult mice. The data shown here reveal incipient dendritogenesis and complete absence of glutamatergic inputs in 21-dpi GCs generated in middle-aged mice (Figures 1 and 2). This is in striking contrast to previous studies in young adult mice showing that GCs receive glutamatergic inputs by 14 dpi and already engage in information processing before 28 dpi (Espósito et al., 2005; Ge et al., 2006; Gu

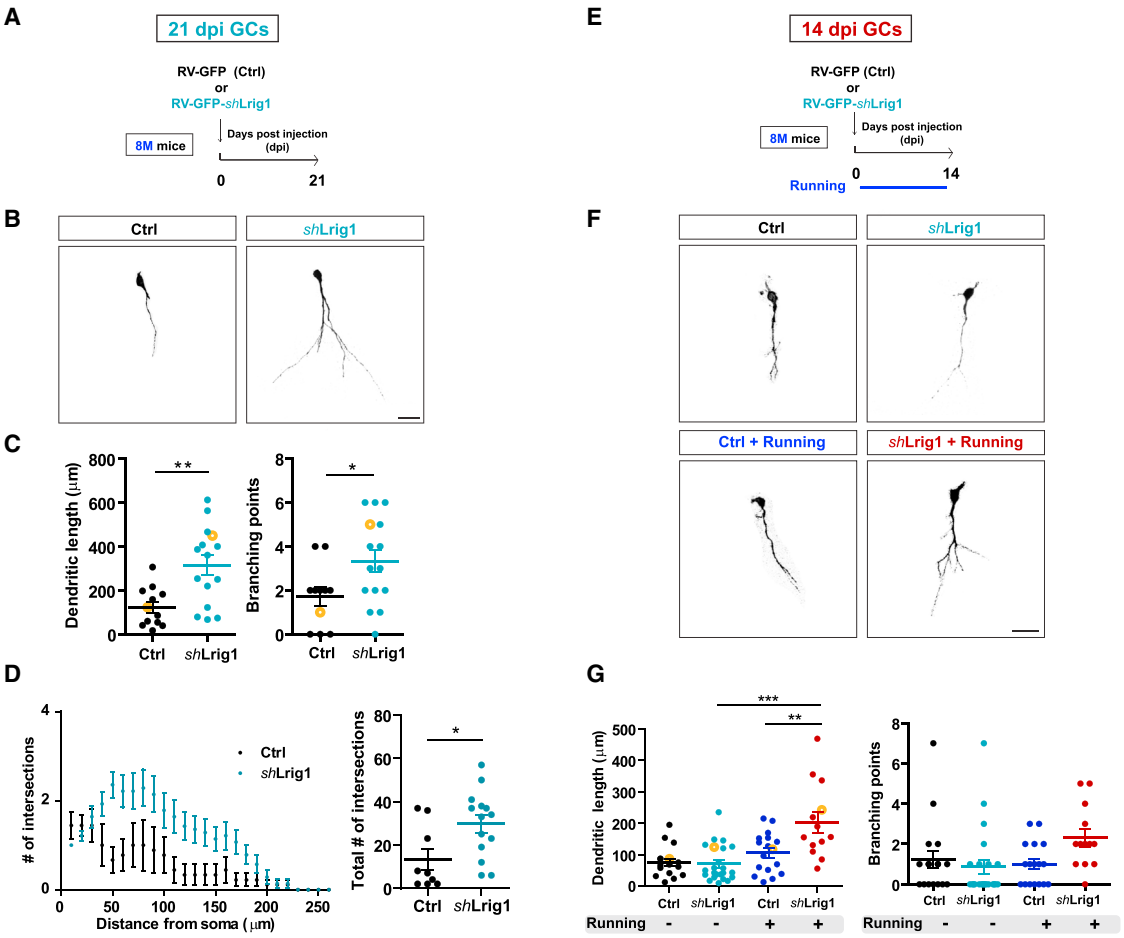

Figure 4. Neurotrophin Receptor Activation by Lrig1 Downregulation Facilitates Accelerated Neuronal Development and Potentiates the Effect of Running in 8M Mice

(A–D) Lrig1 downregulation promotes neuronal growth. (A) Experimental design. RV-GFP-*sh*Lrig1 or RV-GFP (Ctrl) were delivered to the dentate gyrus of 8M mice to transduce new GCs. Morphological analysis was done at 21 dpi. (B) Representative confocal images of 21-dpi GCs. Scale bar, 20 μm. Individual neurons have been cropped from original images. (C and D) Dendritic measurements (C) and Sholl analysis (D) of GFP-GCs. *p < 0.05 and **p < 0.01 after t test with Welch's correction, with n = 12 (Ctrl) and 15 GCs (shLrig1) from 3 and 4 mice.

(E–G) Increased availability of TrkB potentiates the effect of running. (E) Experimental design. RV-*sh*Lrig1-GFP or GFP was used to transduce new GCs. Mice were housed in control cages or with a running wheel. Analysis was done on GFP-GCs at 14 dpi. (F) Confocal images of 21-dpi GCs at the indicated conditions. Scale bar, 20 μm. (G) Dendritic measurements. **p < 0.01 and ***p < 0.001 after Kruskal-Wallis followed by Dunn's post hoc test, with n = 17 (Ctrl), 23 (*sh*Lrig1), 17 (Run) and 13 GCs (Run + *sh*Lrig1) from 3 to 4 mice.

Horizontal and error bars denote mean ± SEM.

et al., 2012; Marín-Burgin et al., 2012; Mongiat et al., 2009; Overstreet-Wadiche et al., 2006).

The protracted integration described earlier was only observed in sedentary mice, where neurons are kept at a state of enhanced sensitivity to activity due to the high electrical input resistance. Voluntary exercise unearthed a remarkable potential for plasticity in new GCs, which displayed dendritic length and spine density similar to the plateau levels found in mature GCs of young adult mice (compare Figures 2E and 2G with Figures 1D and 1F). We also found that intrinsic electrical activity and neurotrophins play fundamental roles in exposing the latent activity-dependent structural plasticity enclosed in young immature GCs in the aging brain. This is consistent with the observations that chronic exercise training increases serum levels of neurotrophic factors, improves memory, and prevents the age-dependent reduction in the volume of the human hippocampus (Duzel et al., 2016; Erickson et al., 2011; Mattson, 2012).

While activity and neurotrophins "rejuvenate" the behavior of new GCs in middle-aged mice, the mechanisms underlying the extended duration of immature neuronal stages remain to be further investigated. It is likely, though, that decreased neuronal activity, oxidative stress, inflammatory niche, and reduced neurotrophic support already described in the aging brain all contribute to the slow development observed in the aging brain (Bishop et al., 2010; Guarente, 2014; Hattiangady et al., 2005; Lee et al., 2000; Verbitsky et al., 2004).

The extended duration of morpho-functional development might be one additional factor contributing to the overall decline

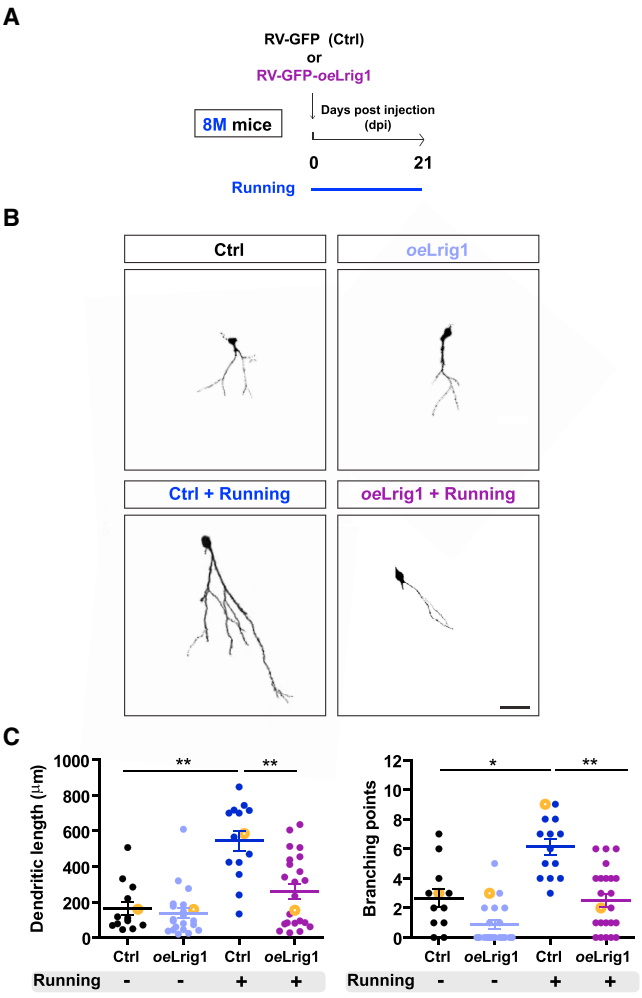

Figure 5. Attenuation of Neurotrophin Signaling by Lrig1 Overexpression Precludes the Effects of Running on Developing GCs

(A) Experimental design. RV-GFP-oeLrig1 or RV-GFP (Ctrl) was delivered to the dentate gyrus of 8M mice. Mice were housed in control cages or with a running wheel. Morphological analysis was done at 21 dpi.

(B) Confocal images. Scale bar, 20 μm.

(C) Dendritic measurements. *$p < 0.05$ and **$p < 0.01$ after Kruskal-Wallis followed by Dunn's post hoc test, with n = 12 (Ctrl), 21 (oeLrig1), 14 (Running), and 23 GCs (Run + oeLrig1) from 3–4 mice. Horizontal and error bars denote mean ± SEM.

of the aging brain. Alternatively, prolonged immature stages during which neurons remain highly sensitive to activity-dependent integration (Alvarez et al., 2016; Bergami et al., 2015; Chancey et al., 2013; Ge et al., 2007; Piatti et al., 2011; Tashiro et al., 2007) might provide additional adaptive value to each newly generated cell: because survival seems to depend on activity-dependent competition (Tashiro et al., 2006), extending the period of high plasticity would increase the chance for survival. Thus, new GCs might remain dormant, and immature until bouts of activity occur (recruitment by demand); then, fast integration and synaptic remodeling would contribute to their integration in a manner that is relevant to information processing.

The trophic effect that exercise exerted on new GCs in aging mice can be dissected as the combination of external signals and their intrinsic mediators, which allow the neuron to respond to them. We found that 2-week-old GCs do not respond to running, unless such response is allowed by increasing Trk receptor availability using Lrig1 knockdown. Thus, availability of Lrig1 targets act in a permissive manner for the actions of physical exercise, linking activity to neuronal growth. By the third week, new GCs respond to exercise, revealing an acquired sensitivity to neurotrophic signaling. The involvement of neurotrophins was demonstrated by the observation that Lrig1 overexpression abolishes the acceleration of neuronal development induced by running.

Whether this mechanism of plasticity contributes to the improved performance in spatial learning reported after exercise in the aging brain is yet to be demonstrated (Duzel et al., 2016; Marlatt et al., 2012; van Praag et al., 2005; Xu et al., 2017). Because adult-born neurons are thought to contribute to spatial tasks involving the discrimination of subtle differences rather than general processing of spatial information, testing their role in the aging brain becomes particularly challenging (Clelland et al., 2009; Drew et al., 2013; McAvoy et al., 2016; Sahay et al., 2011). Finally, given that aging renders the brain vulnerable, understanding the dynamics of activity-dependent network remodeling throughout life is critical for tackling cognitive decline during aging and age-related neurodegeneration (Mattson, 2012).

EXPERIMENTAL PROCEDURES

Production of Viral Vectors

A replication-deficient retroviral vector based on the Moloney murine leukemia virus was used to specifically transduce adult-born GCs as done previously (Temprana et al., 2015). Retroviral particles were assembled using three separate plasmids containing the capside (CMV-vsvg), viral proteins (CMV-gag/pol), and the transgenes: CAG-RFP, CAG-GFP, and EGFP fused to channelrhodopsin-2 (ChR2; Ubi-ChR2-EGFP retroviral plasmid, kindly provided by S. Ge, SUNY at Stony Brook), mouse Lrig1-shRNA-GFP expression vector (Alsina et al., 2016), or the synthetic G-coupled receptor hM3Dq (CAG-EGFP-2A-hM3D) (Alexander et al., 2009), kindly provided by B. Roth (University of North Carolina at Chapel Hill). Plasmids were transfected onto HEK293T cells using deacylated polyethylenimine. HEK293T cells were cultured in DMEM with high glucose, supplemented with 10% fetal calf serum and 2 mM glutamine. Virus-containing supernatant was harvested 48 hr after transfection and concentrated by two rounds of ultracentrifugation. Virus titer was typically ~10^5 particles per microliter.

Mice and Stereotaxic Surgery for Retroviral Delivery

Female C57BL/6J (2, 5, or 8 months of age) and genetically modified mice (12 months of age) were housed at four to five mice per cage in standard conditions. Middle-aged mice were selected because, beyond this age, there is a strong decline in dentate neurogenesis that prevents the study of retrovirally labeled neurons (Morgenstern et al., 2008). $Ascl1^{CreERT2}$ (*Ascl1*$^{tm1(Cre/ERT2)Jejo}$/J) mice (Kim et al., 2007) were crossed to a $CAG^{floxStop\text{-}tdTomato}$ (Ai14) (B6;129S6-*Gt(ROSA)26Sor*$^{tm14(CAG\text{-}tdTomato)Hze}$/J) conditional reporter line (Madisen et al., 2010) to generate $Ascl1^{CreERT2}$; $CAG^{floxStopTom}$ mice, which can be used to reliably target adult-born GCs (Yang et al., 2015). Tamoxifen (TAM) administration (120 μg/g, three injections in 3 days) was carried out in 12M mice to achieve indelible expression of tdTomato (Tom) in the progeny of $Ascl1^+$ progenitor cells. Two to 3 days before TAM induction or retroviral injection, running mice were provided with running wheels (one for every two mice) to maximize the number of labeled adult-born GCs.

Mice were anesthetized (150 μg ketamine/15 μg xylazine in 10 μL saline per gram), and retrovirus was infused into the septal region of the right dentate gyrus (1.5 μL at 0.15 μL/min) using sterile calibrated microcapillary pipettes through stereotaxic surgery coordinates from bregma (in millimeters): −2 anteroposterior, −1.5 lateral, and −1.9 ventral. Brain sections were obtained at the indicated times for confocal imaging. Only neurons in the septal dentate gyrus were included in the analysis, corresponding to sections containing the septal region of the hippocampus (−0.96 to −2.30 mm from the bregma) according to Paxinos and Franklin's mouse brain atlas (Paxinos and Franklin, 2001). Experimental protocols were approved by the Institutional Animal Care and Use Committee of the Fundación Instituto Leloir according to the Principles for Biomedical Research involving animals of the Council for International Organizations for Medical Sciences and provisions stated in the Guide for the Care and Use of Laboratory Animals.

In Vivo Assays

Running

Mice received a stereotaxic injection in the dentate gyrus and were housed with a running wheel for 14 or 21 days (as indicated), where they ran about 10–20 km/night. Mice were then perfused for immunofluorescence analysis. Control mice were left in a regular cage without a running wheel.

EE Exposure

After stereotaxic injection, mice were exposed to an EE consisting of a larger cage (75 cm × 40 cm × 15 cm) with several tunnels and toys (but no running wheel) for 21 days. EE was changed once a week to maintain novelty. Animals were then perfused for immunofluorescence analysis. Control mice were left in the regular cage.

Chemogenetic Activation of New GCs

Mice received the RV-hM3D-EGFP in the right dentate gyrus. CNO administration (1–5 g/g) was done for 21 days in the drinking water.

Immunofluorescence

Immunostaining was done on 60-μm free-floating coronal sections. Antibodies were applied in Tris-buffered saline (TBS) with 3% donkey serum and 0.25% Triton X-100. Double- or triple-labeling immunofluorescence was performed using the following primary antibodies: Arc (rabbit polyclonal; 1:500; Synaptic Systems), calbindin D-28k (rabbit polyclonal; 1:1,000; Swant), GFP (chicken polyclonal; 1:500; Aves), GFP (rabbit polyclonal; 1:500; Invitrogen), NeuN (mouse monoclonal; 1:50; a gift from F.H. Gage, Salk Institute for Biological Studies, La Jolla, CA), and RFP (rabbit polyclonal; 1:500; Rockland Immunochemicals). The following corresponding secondary antibodies were used: donkey anti-mouse Cy5, donkey anti-rabbit Cy3, and donkey anti-chicken Cy2 (1:250; Jackson ImmunoResearch Laboratories).

Confocal Microscopy

Images were acquired using confocal microscopes. For analysis of Arc expression, images were acquired (40×; NA, 1.3; oil immersion), and colocalization was assessed in *Z* stacks using multiple planes for each cell. For dendritic length measurements, images were acquired (40×; NA, 1.3; oil-immersion) from 60-μm-thick sections taking *Z* stacks including 35–50 optical slices, Airy unit = 1 at 0.8-μm intervals. For chemogenetic experiments carried out in 2M and 5M mice, dendritic trees of EGFP-hM3D-GCs were characterized after coinfection with a RV-RFP in a 2:1 ratio to optimize fluorescence detection. Only GCs expressing both EGFP and RFP in their soma were analyzed. For 8M mice, RV-EGFP-hM3 was injected, and dendritic length was measured in GFP^+ neurons. Dendritic length was then measured from projections of three-dimensional reconstructions onto a single plane in GCs expressing both RFP and EGFP in their soma. For Sholl analysis, the ImageJ/Fiji plugin was applied on the same 2D grayscale images used to quantify dendritic length. Total number of intersections was calculated for statistical analyses. For spine counts, images were acquired (63×; NA, 1.4; oil immersion) from 60-μm-thick sections taking *Z* stacks including 50–140 optical slices, Airy unit = 1 at 0.1-μm intervals. Three-dimensional reconstruction of dendritic segments was performed as previously described (Morgenstern et al., 2008). Spines were counted manually from dendritic fragments of >40 μm located in the middle third of the molecular layer. Spine counts were not performed in shLrig1-GCs or HM3D-GCs due to the weak fluorescence expressed by those viral constructs. For image capture and analysis of morphological properties, all experimental groups under study were blind to the operator.

Western Blots

Western blot analysis was performed as previously described (Paratcha et al., 2003). Briefly, hippocampal tissue from 2M, 5M, and 8M sedentary and running mice was dissected and homogenized (10% w/v) in ice-cold 25 mM Tris-HCl (pH 7.4) containing 0.32 M sucrose, 1 mM EDTA, and protease inhibitors. Tissue homogenization was performed by 40 strokes in a glass homogenizer. After centrifugation at 1,000 × *g* for 10 min, the supernatant was analyzed by western blot to evaluate the protein levels of BDNF with anti-BDNF antibody (1:1,000, Santa Cruz) and anti-βIII tubulin (1:5,000, Promega). Immunoblots were examined and analyzed using a fluorescence scanner.

Electrophysiology

Slice Preparation

12M $Ascl1^{CreERT2}$;$CAG^{floxStop\text{-}tdTomato}$ mice were anesthetized and decapitated at 19 to 21 days after TAM induction, as indicated, and transverse slices were prepared as described previously (Alvarez et al., 2016). Briefly, brains were removed into a chilled solution containing (in millimolar): 110 choline-Cl, 2.5 KCl, 2.0 NaH_2PO_4, 25 $NaHCO_3$, 0.5 $CaCl_2$, 7 $MgCl_2$, 20 dextrose, 1.3 Na^+-ascorbate, 3.1 Na^+-pyruvate, and 4 kynurenic acid (kyn). Coronal slices (400 μm thick) from the septal pole containing both hippocampi were cut with a vibratome and transferred to a chamber containing (in millimolar): 125 NaCl, 2.5 KCl, 2 NaH_2PO_4, 25 $NaHCO_3$, 2 $CaCl_2$, 1.3 $MgCl_2$, 1.3 Na^+-ascorbate, 3.1 Na^+-pyruvate, and 10 dextrose (315 mOsm). Slices were bubbled with 95% O_2/5% CO_2 and maintained at 30°C for >45 min before experiments started.

Recordings

Whole-cell recordings were performed using microelectrodes (4–6 MΩ) filled with (in millimolar): 150 K-gluconate, 1 NaCl, 4 $MgCl_2$, 0.1 EGTA, 10 HEPES, 4 ATP-Tris, 0.3 GTP-Tris, and 10 phosphocreatine, in the presence of picrotoxin (PTX; 100 μM). Criteria to include cells in the analysis were visual confirmation of Tom in the pipette tip, attachment of the labeled soma to the pipette when suction was performed, and absolute leak current <100 pA at holding potential (V_h). Spontaneous EPSCs were recorded in voltage clamp at −70 mV. Input resistance was assessed by the application of voltage steps of 10 mV in voltage-clamp mode, and spiking by the injection of current steps (10 pA) in current-clamp configuration after taking the membrane potential to −70 mV. All recordings were performed at room temperature (23°C ± 2°C), digitized, and acquired at 10 KHz on a personal computer. Detection and analysis of spontaneous EPSCs was done using a dedicated software package.

Statistical Analysis

Statistics used throughout the paper are described in the figure legends and in the text. Unless otherwise specified, data are presented as mean ± SEM. Normality was assessed using the Shapiro-Wilks test, D'Agostino-Pearson omnibus test, and Kolmogorov-Smirnov test, with a P value of 0.05. When data met normality tests (Gaussian distribution and equal variance), an unpaired t test with Welch's correction or an ANOVA with Bonferroni's post hoc test was used as indicated. In cases in which data did not meet normality criteria, nonparametric tests were used as follows: Mann-Whitney test for independent comparisons, and Kruskal-Wallis test for multiple comparisons.

SUPPLEMENTAL INFORMATION

Supplemental Information includes four figures and can be found with this article online at https://doi.org/10.1016/j.celrep.2017.09.064.

AUTHOR CONTRIBUTIONS

M.F.T. is the lead author, contributed to the concept, designed, and performed the experiments, analyzed the data, and wrote the manuscript. K.A.B. and J.N.S.C. performed immunofluorescence and confocal image data collection

and analysis. S.G.T. performed electrophysiological recordings. P.A.F. performed western blots. M.C.M.-S. prepared all retroviruses and helped in processing brain samples. F.L. and G.P. contributed to neurotrophin signaling experiments and provided insightful ideas. A.F.S. contributed to the concept, designed the experiments, analyzed the data, wrote the manuscript, and provided financial support.

ACKNOWLEDGMENTS

We thank Jane Johnson for Ascl1CreERT2 mice, Bryan Roth for the hM3D construct, members of the A.F.S. lab and the Guillermo Lanuza lab for insightful discussions, and M. Fernanda Ceriani for critical comments on the manuscript. F.L., G.P., and A.F.S. are investigators of the Consejo Nacional de Investigaciones Científicas y Técnicas (CONICET). M.F.T., S.G.T., and P.A.F. were supported by CONICET fellowships. This work was supported by grants from the Argentine Agency for the Promotion of Science and Technology (PICT2015-3814 to F.L. and A.F.S. and PICT2013-1685 to A.F.S.) and the Howard Hughes Medical Institute (SIRS grant no. 55007652) to A.F.S.

Received: June 20, 2017
Revised: August 23, 2017
Accepted: September 19, 2017
Published: October 31, 2017

REFERENCES

Adlard, P.A., Perreau, V.M., and Cotman, C.W. (2005). The exercise-induced expression of BDNF within the hippocampus varies across life-span. Neurobiol. Aging *26*, 511–520.

Alexander, G.M., Rogan, S.C., Abbas, A.I., Armbruster, B.N., Pei, Y., Allen, J.A., Nonneman, R.J., Hartmann, J., Moy, S.S., Nicolelis, M.A., et al. (2009). Remote control of neuronal activity in transgenic mice expressing evolved G protein-coupled receptors. Neuron *63*, 27–39.

Alsina, F.C., Hita, F.J., Fontanet, P.A., Irala, D., Hedman, H., Ledda, F., and Paratcha, G. (2016). Lrig1 is a cell-intrinsic modulator of hippocampal dendrite complexity and BDNF signaling. EMBO Rep. *17*, 601–616.

Alvarez, D.D., Giacomini, D., Yang, S.M., Trinchero, M.F., Temprana, S.G., Büttner, K.A., Beltramone, N., and Schinder, A.F. (2016). A disynaptic feedback network activated by experience promotes the integration of new granule cells. Science *354*, 459–465.

Beckervordersandforth, R., Ebert, B., Schaffner, I., Moss, J., Fiebig, C., Shin, J., Moore, D.L., Ghosh, L., Trinchero, M.F., Stockburger, C., et al. (2017). Role of mitochondrial metabolism in the control of early lineage progression and aging phenotypes in adult hippocampal neurogenesis. Neuron *93*, 560–573.e56.

Bergami, M., Rimondini, R., Santi, S., Blum, R., Götz, M., and Canossa, M. (2008). Deletion of TrkB in adult progenitors alters newborn neuron integration into hippocampal circuits and increases anxiety-like behavior. Proc. Natl. Acad. Sci. USA *105*, 15570–15575.

Bergami, M., Masserdotti, G., Temprana, S.G., Motori, E., Eriksson, T.M., Göbel, J., Yang, S.M., Conzelmann, K.K., Schinder, A.F., Götz, M., and Berninger, B. (2015). A critical period for experience-dependent remodeling of adult-born neuron connectivity. Neuron *85*, 710–717.

Bishop, N.A., Lu, T., and Yankner, B.A. (2010). Neural mechanisms of ageing and cognitive decline. Nature *464*, 529–535.

Bonaguidi, M.A., Wheeler, M.A., Shapiro, J.S., Stadel, R.P., Sun, G.J., Ming, G.L., and Song, H. (2011). In vivo clonal analysis reveals self-renewing and multipotent adult neural stem cell characteristics. Cell *145*, 1142–1155.

Burke, S.N., and Barnes, C.A. (2010). Senescent synapses and hippocampal circuit dynamics. Trends Neurosci. *33*, 153–161.

Chancey, J.H., Adlaf, E.W., Sapp, M.C., Pugh, P.C., Wadiche, J.I., and Overstreet-Wadiche, L.S. (2013). GABA depolarization is required for experience-dependent synapse unsilencing in adult-born neurons. J. Neurosci. *33*, 6614–6622.

Cheung, Z.H., Chin, W.H., Chen, Y., Ng, Y.P., and Ip, N.Y. (2007). Cdk5 is involved in BDNF-stimulated dendritic growth in hippocampal neurons. PLoS Biol. *5*, e63.

Clelland, C.D., Choi, M., Romberg, C., Clemenson, G.D., Jr., Fragniere, A., Tyers, P., Jessberger, S., Saksida, L.M., Barker, R.A., Gage, F.H., and Bussey, T.J. (2009). A functional role for adult hippocampal neurogenesis in spatial pattern separation. Science *325*, 210–213.

Corenblum, M.J., Ray, S., Remley, Q.W., Long, M., Harder, B., Zhang, D.D., Barnes, C.A., and Madhavan, L. (2016). Reduced Nrf2 expression mediates the decline in neural stem cell function during a critical middle-age period. Aging Cell *15*, 725–736.

Drew, L.J., Fusi, S., and Hen, R. (2013). Adult neurogenesis in the mammalian hippocampus: why the dentate gyrus? Learn. Mem. *20*, 710–729.

Duzel, E., van Praag, H., and Sendtner, M. (2016). Can physical exercise in old age improve memory and hippocampal function? Brain *139*, 662–673.

Encinas, J.M., Michurina, T.V., Peunova, N., Park, J.H., Tordo, J., Peterson, D.A., Fishell, G., Koulakov, A., and Enikolopov, G. (2011). Division-coupled astrocytic differentiation and age-related depletion of neural stem cells in the adult hippocampus. Cell Stem Cell *8*, 566–579.

Erickson, K.I., Voss, M.W., Prakash, R.S., Basak, C., Szabo, A., Chaddock, L., Kim, J.S., Heo, S., Alves, H., White, S.M., et al. (2011). Exercise training increases size of hippocampus and improves memory. Proc. Natl. Acad. Sci. USA *108*, 3017–3022.

Espósito, M.S., Piatti, V.C., Laplagne, D.A., Morgenstern, N.A., Ferrari, C.C., Pitossi, F.J., and Schinder, A.F. (2005). Neuronal differentiation in the adult hippocampus recapitulates embryonic development. J. Neurosci. *25*, 10074–10086.

Fan, X., Wheatley, E.G., and Villeda, S.A. (2017). Mechanisms of hippocampal aging and the potential for rejuvenation. Annu. Rev. Neurosci. *40*, 251–272.

Ge, S., Goh, E.L., Sailor, K.A., Kitabatake, Y., Ming, G.L., and Song, H. (2006). GABA regulates synaptic integration of newly generated neurons in the adult brain. Nature *439*, 589–593.

Ge, S., Yang, C.H., Hsu, K.S., Ming, G.L., and Song, H. (2007). A critical period for enhanced synaptic plasticity in newly generated neurons of the adult brain. Neuron *54*, 559–566.

Gu, Y., Arruda-Carvalho, M., Wang, J., Janoschka, S.R., Josselyn, S.A., Frankland, P.W., and Ge, S. (2012). Optical controlling reveals time-dependent roles for adult-born dentate granule cells. Nat. Neurosci. *15*, 1700–1706.

Guarente, L. (2014). Aging research-where do we stand and where are we going? Cell *159*, 15–19.

Hattiangady, B., Rao, M.S., Shetty, G.A., and Shetty, A.K. (2005). Brain-derived neurotrophic factor, phosphorylated cyclic AMP response element binding protein and neuropeptide Y decline as early as middle age in the dentate gyrus and CA1 and CA3 subfields of the hippocampus. Exp. Neurol. *195*, 353–371.

Irwin, D.J., Lee, V.M., and Trojanowski, J.Q. (2013). Parkinson's disease dementia: convergence of α-synuclein, tau and amyloid-β pathologies. Nat. Rev. Neurosci. *14*, 626–636.

Kempermann, G., Kuhn, H.G., and Gage, F.H. (1998). Experience-induced neurogenesis in the senescent dentate gyrus. J. Neurosci. *18*, 3206–3212.

Kim, E.J., Leung, C.T., Reed, R.R., and Johnson, J.E. (2007). In vivo analysis of Ascl1 defined progenitors reveals distinct developmental dynamics during adult neurogenesis and gliogenesis. J. Neurosci. *27*, 12764–12774.

Knobloch, M., Braun, S.M., Zurkirchen, L., von Schoultz, C., Zamboni, N., Araúzo-Bravo, M.J., Kovacs, W.J., Karalay, O., Suter, U., Machado, R.A., et al. (2013). Metabolic control of adult neural stem cell activity by Fasn-dependent lipogenesis. Nature *493*, 226–230.

Kropff, E., Yang, S.M., and Schinder, A.F. (2015). Dynamic role of adult-born dentate granule cells in memory processing. Curr. Opin. Neurobiol. *35*, 21–26.

Kuhn, H.G., Dickinson-Anson, H., and Gage, F.H. (1996). Neurogenesis in the dentate gyrus of the adult rat: age-related decrease of neuronal progenitor proliferation. J. Neurosci. *16*, 2027–2033.

Kuipers, S.D., Schroeder, J.E., and Trentani, A. (2015). Changes in hippocampal neurogenesis throughout early development. Neurobiol. Aging *36*, 365–379.

Lee, C.K., Weindruch, R., and Prolla, T.A. (2000). Gene-expression profile of the ageing brain in mice. Nat. Genet. *25*, 294–297.

Lepousez, G., Nissant, A., and Lledo, P.M. (2015). Adult neurogenesis and the future of the rejuvenating brain circuits. Neuron *86*, 387–401.

López-Otín, C., Blasco, M.A., Partridge, L., Serrano, M., and Kroemer, G. (2013). The hallmarks of aging. Cell *153*, 1194–1217.

Madisen, L., Zwingman, T.A., Sunkin, S.M., Oh, S.W., Zariwala, H.A., Gu, H., Ng, L.L., Palmiter, R.D., Hawrylycz, M.J., Jones, A.R., et al. (2010). A robust and high-throughput Cre reporting and characterization system for the whole mouse brain. Nat. Neurosci. *13*, 133–140.

Marín-Burgin, A., Mongiat, L.A., Pardi, M.B., and Schinder, A.F. (2012). Unique processing during a period of high excitation/inhibition balance in adult-born neurons. Science *335*, 1238–1242.

Marlatt, M.W., Potter, M.C., Lucassen, P.J., and van Praag, H. (2012). Running throughout middle-age improves memory function, hippocampal neurogenesis, and BDNF levels in female C57BL/6J mice. Dev. Neurobiol. *72*, 943–952.

Mattson, M.P. (2012). Energy intake and exercise as determinants of brain health and vulnerability to injury and disease. Cell Metab. *16*, 706–722.

McAllister, A.K., Katz, L.C., and Lo, D.C. (1996). Neurotrophin regulation of cortical dendritic growth requires activity. Neuron *17*, 1057–1064.

McAvoy, K.M., Scobie, K.N., Berger, S., Russo, C., Guo, N., Decharatanachart, P., Vega-Ramirez, H., Miake-Lye, S., Whalen, M., Nelson, M., et al. (2016). Modulating neuronal competition dynamics in the dentate gyrus to rejuvenate aging memory circuits. Neuron *91*, 1356–1373.

Meyer-Franke, A., Wilkinson, G.A., Kruttgen, A., Hu, M., Munro, E., Hanson, M.G., Jr., Reichardt, L.F., and Barres, B.A. (1998). Depolarization and cAMP elevation rapidly recruit TrkB to the plasma membrane of CNS neurons. Neuron *21*, 681–693.

Mongiat, L.A., Espósito, M.S., Lombardi, G., and Schinder, A.F. (2009). Reliable activation of immature neurons in the adult hippocampus. PLoS ONE *4*, e5320.

Moore, D.L., Pilz, G.A., Araúzo-Bravo, M.J., Barral, Y., and Jessberger, S. (2015). A mechanism for the segregation of age in mammalian neural stem cells. Science *349*, 1334–1338.

Morgenstern, N.A., Lombardi, G., and Schinder, A.F. (2008). Newborn granule cells in the ageing dentate gyrus. J. Physiol. *586*, 3751–3757.

Oliff, H.S., Berchtold, N.C., Isackson, P., and Cotman, C.W. (1998). Exercise-induced regulation of brain-derived neurotrophic factor (BDNF) transcripts in the rat hippocampus. Brain Res. Mol. Brain Res. *61*, 147–153.

Overstreet-Wadiche, L.S., Bensen, A.L., and Westbrook, G.L. (2006). Delayed development of adult-generated granule cells in dentate gyrus. J. Neurosci. *26*, 2326–2334.

Paratcha, G., Ledda, F., and Ibáñez, C.F. (2003). The neural cell adhesion molecule NCAM is an alternative signaling receptor for GDNF family ligands. Cell *113*, 867–879.

Park, H., and Poo, M.M. (2013). Neurotrophin regulation of neural circuit development and function. Nat. Rev. Neurosci. *14*, 7–23.

Paxinos, G., and Franklin, K.B.J. (2001). The Mouse Brain in Stereotaxic Coordinates (Academic Press).

Piatti, V.C., Davies-Sala, M.G., Espósito, M.S., Mongiat, L.A., Trinchero, M.F., and Schinder, A.F. (2011). The timing for neuronal maturation in the adult hippocampus is modulated by local network activity. J. Neurosci. *31*, 7715–7728.

Sahay, A., Scobie, K.N., Hill, A.S., O'Carroll, C.M., Kheirbek, M.A., Burghardt, N.S., Fenton, A.A., Dranovsky, A., and Hen, R. (2011). Increasing adult hippocampal neurogenesis is sufficient to improve pattern separation. Nature *472*, 466–470.

Sierra, A., Martín-Suárez, S., Valcárcel-Martín, R., Pascual-Brazo, J., Aelvoet, S.A., Abiega, O., Deudero, J.J., Brewster, A.L., Bernales, I., Anderson, A.E., et al. (2015). Neuronal hyperactivity accelerates depletion of neural stem cells and impairs hippocampal neurogenesis. Cell Stem Cell *16*, 488–503.

Sternson, S.M., and Roth, B.L. (2014). Chemogenetic tools to interrogate brain functions. Annu. Rev. Neurosci. *37*, 387–407.

Tashiro, A., Sandler, V.M., Toni, N., Zhao, C., and Gage, F.H. (2006). NMDA-receptor-mediated, cell-specific integration of new neurons in adult dentate gyrus. Nature *442*, 929–933.

Tashiro, A., Makino, H., and Gage, F.H. (2007). Experience-specific functional modification of the dentate gyrus through adult neurogenesis: a critical period during an immature stage. J. Neurosci. *27*, 3252–3259.

Temprana, S.G., Mongiat, L.A., Yang, S.M., Trinchero, M.F., Alvarez, D.D., Kropff, E., Giacomini, D., Beltramone, N., Lanuza, G.M., and Schinder, A.F. (2015). Delayed coupling to feedback inhibition during a critical period for the integration of adult-born granule cells. Neuron *85*, 116–130.

van Praag, H., Christie, B.R., Sejnowski, T.J., and Gage, F.H. (1999). Running enhances neurogenesis, learning, and long-term potentiation in mice. Proc. Natl. Acad. Sci. USA *96*, 13427–13431.

van Praag, H., Shubert, T., Zhao, C., and Gage, F.H. (2005). Exercise enhances learning and hippocampal neurogenesis in aged mice. J. Neurosci. *25*, 8680–8685.

Verbitsky, M., Yonan, A.L., Malleret, G., Kandel, E.R., Gilliam, T.C., and Pavlidis, P. (2004). Altered hippocampal transcript profile accompanies an age-related spatial memory deficit in mice. Learn. Mem. *11*, 253–260.

Villeda, S.A., Luo, J., Mosher, K.I., Zou, B., Britschgi, M., Bieri, G., Stan, T.M., Fainberg, N., Ding, Z., Eggel, A., et al. (2011). The ageing systemic milieu negatively regulates neurogenesis and cognitive function. Nature *477*, 90–94.

Wang, L., Chang, X., She, L., Xu, D., Huang, W., and Poo, M.M. (2015). Autocrine action of BDNF on dendrite development of adult-born hippocampal neurons. J. Neurosci. *35*, 8384–8393.

Waterhouse, E.G., An, J.J., Orefice, L.L., Baydyuk, M., Liao, G.Y., Zheng, K., Lu, B., and Xu, B. (2012). BDNF promotes differentiation and maturation of adult-born neurons through GABAergic transmission. J. Neurosci. *32*, 14318–14330.

Xu, B., Sun, A., He, Y., Qian, F., Liu, L., Chen, Y., and Luo, H. (2017). Running-induced memory enhancement correlates with the preservation of thin spines in the hippocampal area CA1 of old C57BL/6 mice. Neurobiol. Aging *52*, 106–116.

Yang, S.M., Alvarez, D.D., and Schinder, A.F. (2015). Reliable genetic labeling of adult-born dentate granule cells using Ascl1 CreERT2 and Glast CreERT2 murine lines. J. Neurosci. *35*, 15379–15390.

Zhao, C., Teng, E.M., Summers, R.G., Jr., Ming, G.L., and Gage, F.H. (2006). Distinct morphological stages of dentate granule neuron maturation in the adult mouse hippocampus. J. Neurosci. *26*, 3–11.